

# Adenovirus-mediated P311 inhibits TGF- $\beta$ 1-induced epithelial-mesenchymal transition in NRK-52E cells *via* TGF- $\beta$ 1-Smad-ILK pathway

Fanghua Qi<sup>1</sup>, Pingping Cai<sup>1</sup>, Xiang Liu<sup>2</sup>, Min Peng<sup>1</sup>, Guomin Si<sup>1,\*</sup>

<sup>1</sup> Department of Traditional Chinese Medicine, Shandong Provincial Hospital affiliated to Shandong University, Ji'nan, China;

<sup>2</sup> Department of Nephrology, Shandong Provincial Hospital affiliated to Shandong University, Ji'nan, China.

## Summary

P311, a highly conserved 8-kDa intracellular protein, has been indicated as an important factor in myofibroblast transformation and in the progression of fibrosis. In the present study, we constructed a recombinant adenovirus vector of p311 (called Ad-P311) and transferred it into rat renal proximal tubular epithelial cells (NRK-52E) to explore the effect of P311 on epithelial-mesenchymal transition (EMT) of NRK-52E cells induced by TGF- $\beta$ 1 and to elucidate its underlying mechanism against EMT. After successfully construction of Ad-P311 and transfer into NRK-52E cells, the proliferation and growth of P311-expressing cells was detected by MTT assay. TGF- $\beta$ 1 was used to induce NRK-52E cells and Western blot analysis was used to examine the EMT markers (E-cadherin and  $\alpha$ -smooth muscle actin ( $\alpha$ -SMA)), signal transducers (p-Smad2/3 and Smad7). Integrin Linked Kinase (ILK) as a key intracellular mediator that controls TGF- $\beta$ 1-induced-EMT was also assayed by Western blot analysis. The results showed that P311 transfection could significantly inhibit the proliferation and growth of TGF- $\beta$ 1 induced NRK-52E cells. The results also showed that TGF- $\beta$ 1 could induce EMT in NRK-52E cells through Smad-ILK signaling pathway with an increase in  $\alpha$ -SMA, pSmad2/3 and ILK expression, and a decrease in E-cadherin and Smad7 expression. However, P311 efficiently blocked Smad-ILK pathway activation and attenuated all these EMT changes induced by TGF- $\beta$ 1. These findings suggest that P311 might be involved in the pathogenesis of renal fibrosis by inhibiting the EMT process *via* TGF- $\beta$ 1-Smad-ILK pathway. P311 might be a novel target for the control of renal fibrosis and the progression of CKD.

**Keywords:** Renal fibrosis, P311, TGF- $\beta$ 1, epithelial-mesenchymal transition (EMT), NRK-52E cells

## 1. Introduction

Chronic kidney disease (CKD) has been recognized as a worldwide health issue because of its high prevalence and the accompanying increase in the risk of end-stage renal disease, cardiovascular events, and premature death (1). Renal fibrosis is a pivotal event in the progression of CKD, which is characterized by the deposition of extracellular matrix (ECM) (2).

ECM is thought to be produced by myofibroblasts. Epithelial-mesenchymal transition (EMT) of tubular epithelial cells into myofibroblasts is one of the critical pathogenic mechanisms of renal fibrosis (3). During the EMT process, epithelial cells lose their polarity and epithelial surface markers such as E-cadherin, and acquire mesenchymal features such as  $\alpha$ -smooth muscle actin ( $\alpha$ -SMA) (4). Preventing EMT could ameliorate renal fibrosis and delay the progression of CKD.

Increasing evidence suggests that the EMT of renal tubules is regulated by different growth factors, cytokines, hormones and extracellular signals (5). TGF- $\beta$ 1 is regarded as one of the most important cytokines which regulates the transdifferentiation of tubular epithelial cells into myofibroblasts in renal

\*Address correspondence to:

Dr. Guomin Si, Department of Traditional Chinese Medicine, Shandong Provincial Hospital affiliated to Shandong University, No. 324, Jingwuweiqi Road, Ji'nan 250021, Shandong, China.  
E-mail: sgm977@126.com

fibrosis. It has been shown to initiate and complete the whole EMT process (6). Emerging data indicate that TGF- $\beta$ 1 induced EMT *via* Smad-dependent and Smad-independent pathways. In the Smad-dependent pathway, TGF- $\beta$  signals are transduced by transmembrane serine/threonine kinase type II and type I receptors (7). Upon TGF- $\beta$ 1 binding to its receptors, Serine/Threonine kinases are activated and induce phosphorylation of Smad2/Smad3, then phosphorylate Smad2/3 partners with Smad4 translocated into the nucleus where they regulate the transcription of the target genes responsible for EMT (8). Integrin Linked Kinase (ILK) is an intracellular serine/threonine kinase involved in cell-matrix interactions. It is shown to be a key intracellular mediator that controls TGF- $\beta$ 1-induced-EMT in renal tubular epithelial cells (9). Although the involvement of ILK in tubular EMT has been established by several lines of evidence, intriguingly, many components of ILK signaling, including ILK and  $\beta$ 1-integrin are induced simultaneously by TGF- $\beta$  in a Smad-dependent manner (3,10). Therefore, it is widely accepted that TGF- $\beta$ 1 plays an important role in promoting tubular EMT *via* TGF- $\beta$ 1-Smad-ILK pathway.

P311 is a highly conserved, 8-kDa intracellular protein with a PEST domain abundantly expressed in neurons and muscles (11). It can bind to TGF- $\beta$  latency associated protein and stimulate the translation of TGF- $\beta$  (12). In addition, P311 is detected in myofibroblasts, at the invading edge of glioblastomas, in regenerating nerve and lung, and in hypertrophic scars (13-17). It has been implicated in myofibroblast transformation, cell migration, wound healing, as well as nerve and lung regeneration. Some researchers reported that P311 transfection into fibroblast cells induced phenotypic changes consistent with myofibroblast transformation, decreased TGF- $\beta$ 1 signaling and caused an inhibition of collagen expression. Their findings suggested that P311 might be involved in facilitating wound healing and/or minimizing scarring during wound repair *via* preventing fibrosis (13). A recent study indicated that P311 might be a key cytokine involved in the progression of kidneys of immunoglobulin-A nephropathy (IgAN) (18). However, the related reports about P311 on renal fibrosis are limited and the mechanisms of P311 in the progression of CKD remain largely unknown. Thus, in the present study, we constructed a recombinant adenovirus vector of p311 and transferred it into NRK-52E cells to explore the preventive effect and possible mechanism of P311 on TGF- $\beta$ 1-induced EMT, which might provide new sight for ameliorating renal fibrosis and delaying the progression of CKD.

## 2. Materials and Methods

### 2.1. Cells

Rat renal proximal tubular epithelial cells NRK-52E

and human embryonic kidney cells HEK293A were purchased from the Institute of Biochemistry and Cell Biology (Shanghai, China) and cultured in DMEM (Gibco, CA, USA) with 10% fetal bovine serum (FBS) (Gibco, CA, USA) in an atmosphere of 5% CO<sub>2</sub> at 37°C.

### 2.2. Construction and identification of plasmid

P311 gene adenovirus plasmid was constructed according to previous studies (19). First, according to the sequence of GeneBank, the target gene P311-His\_tag was designed and synthesized with His\_tag sequence and SpeI added at the 3' end and EcoRI added at the 5' end of the P311 gene. Second, both target gene P311-His\_tag and shuttle vector pDown-MCS-IRES/eGFP were digested by EcoRI and SpeI and recovered by agarose gel electrophoresis. Third, the digested products were purified and ligated with T4 DNA ligase and then co-transformed into *E. coli* stb13 cells (Gibco, CA, USA). Thus, the fragment of P311-His\_tag gene was cloned into the shuttle plasmid pDown-MCS-IRES/eGFP (Invitrogen, NY, USA), and the recombinant adenoviral plasmid was generated. Following amplification, the plasmid was extracted and cloned.

### 2.3. Packaging and amplification of the recombinant adenovirus

To package the adenovirus, HEK293A cells were cultured and were inoculated on 6-well plates. The recombinant adenovirus plasmid was digested with PacI and linearized, and was then purified by gel recycling. The linearized plasmid DNA was then transfected into HEK293A cells using Lipofectamine 2000 (Invitrogen, NY, USA) and incubated for 7 days at 37°C as described in the manual. The cells were scraped off the plates and the virus was collected by three consecutive freezing/thawing cycles. To amplify the adenovirus, 1/3 of the obtained virus was used for infection of HEK293A cells, and cells were collected after 48 h. Amplification was repeated as such for a total of four times, all cells were collected, and were then frozen and thawed repeatedly to obtain the recombinant adenovirus. The titer of recombinant adenovirus (called Ad-P311) was detected by TCID50. The control Ad-CMV-eGFP was constructed in the same way. The Ad-P311 and Ad-CMV-eGFP were stored at -80°C for use.

### 2.4. Determination of infection efficiency in NRK-52E cells infected by Ad-P311 *in vitro* and the most optimal MOI

The adenovirus Ad-CMV-eGFP was used as a control and the efficiency of infection was determined by the rate of GFP expression according to standard procedure

and improved according to previous studies (20). Briefly, reconstructed adenovirus (stored at -80 °C) was serially diluted in DMEM without serum and pre-incubated with Lipofectamine 2000 at a final concentration of 1%. The virus-lipid mixture was incubated at 37 °C for 30 min before adding to the NRK-52E cells. NRK-52E cells within three generations were digested with trypsin and mixed, then transferred into 12-well plates at a density of  $1 \times 10^5$  cells/per well with routine culture until firm adherence. Different volumes (2  $\mu$ L, 4  $\mu$ L, 6  $\mu$ L, 8  $\mu$ L, 10  $\mu$ L, and 15  $\mu$ L) of Ad-P311 and Ad-CMV-eGFP were respectively transferred into NRK-52E cells. Following incubation for 8 h (being rocked every 30 min) at 37°C, CO<sub>2</sub>, the cells were routinely cultured for 48 h with complete medium and then observed under the inversion fluorescence microscope. The best multiplicity of infection (MOI) was worked out according to a formula (MOI) = (virus titer)  $\times$  (virus liquid volume)/(cell number for transfection). The largest MOI not causing a marked cytopathic effect (CPE) was considered as the best MOI. The virus liquid was transferred into NRK-52E cells at its best MOI value in the following experiments.

#### 2.5. P311 mRNA expression in NRK-52E Cells infected by Ad-P311

Firstly, NRK-52E cells were infected with Ad-P311 (as described above) for 48h, and then infected NRK-52E cells were collected. The mRNA expression of P311 was detected by quantitative real-time RT-PCR assay (21). The primers for the P311 and GAPDH are shown as follows: P311: forward 5'-AACAAAGGACATGGAGGGAAGG-3' and reverse 5'-TAACTGATTCTTGGGGAGCGG-3'; GAPDH: forward 5'-GGCTCATGACCACAGTCCAT-3' and reverse 5'-TCAGCTCTGGGATGACCTTG-3'. First, total RNA was prepared from the cells using TRIzol (Grand Island, NY, USA) reagent according to the manufacturer's instructions. Then, total RNA was reverse transcribed into cDNA using the SuperScript II First Strand Synthesis System (Grand Island, NY, USA) according to the manufacturer's directions. Afterwards, according to the protocol of SYBR Premix Ex Taq™ kit (TaKaRa Bio Inc., Dalian, China), amplification of target gene and GAPDH were conducted using ABI Prism 7500 Detection System (Applied Biosystems, Inc., USA). The analysis of relative gene expression was performed by comparative 2<sup>- $\Delta\Delta$ CT</sup> method.

#### 2.6. Cell treatment

After infection with adenovirus, cells were treated and divided into six groups as follows: NRK-52E group, NRK-52E/GFP group (infected by Ad-CMV-eGFP), NRK-52E/P311 (infected by Ad-P311), and TGF- $\beta$ 1 (5 ng/mL) induced groups: NRK-52E (TGF- $\beta$ 1) group,

NRK-52E/GFP (TGF- $\beta$ 1) group, and NRK-52E/P311 (TGF- $\beta$ 1) group. NRK-52E group was control group and the other five groups were treatment groups. At the indicated time points, cells were harvested and processed for the following experiments.

#### 2.7. Cell proliferation assay

A MTT (3-[4, 5-dimethylthiazol-2-yl]-2,5-diphenyl-tetrazolium bromide) assay was used to detect cell viability as previously described (22). The cells were cultured at a density of  $6 \times 10^3$  cells/well in triplicate in 96-well plates with TGF- $\beta$ 1 (5 ng/mL) for 7 days and exposed to fresh media and TGF- $\beta$ 1 every other day. MTT assay was performed every day up to the 7th day. Briefly, 20  $\mu$ L of 5 mg/mL MTT (Sigma, St. Louis, MO, USA) was added to each well; plates were incubated at 37°C for 4 h. The generated formazan was dissolved in 150  $\mu$ L dimethyl sulfoxide (DMSO) and measured with a microplate reader (BioRad, Hercules, CA) at an optical density (OD) at 570 nm for determining cell viability. Cell proliferation rate was calculated according to a formula as follows: Cell proliferation rate (%) = OD value of treatment group/OD value of control group  $\times$  100%.

#### 2.8. Western blot analysis

After culturing with TGF- $\beta$ 1 (5 ng/mL) for 48h, total cell lysates and cytosolic fractions were prepared as previously described (21). Thirty micrograms of total cellular proteins were resolved using sodium dodecyl sulfate polyacrylamide gel electrophoresis (SDS PAGE) and transferred onto polyvinylidene fluoride (PVDF) transfer membranes for Western blotting. The results were quantified using Image J (National Institutes of Health, Bethesda, MD, USA). The following antibodies were used: Smad2/3, Smad7,  $\alpha$ -SMA, E-cadherin, ILK, and GAPDH (Santa Cruz Biotechnology, Santa Cruz, CA, USA).

#### 2.9. Statistical analysis

Statistical analysis was performed using SPSS software, version 17.0 (SPSS Inc., USA). The data are expressed as the mean  $\pm$  standard deviation (SD). The statistical significance differences were calculated using the t-test and one-way analysis of variance (ANOVA), and  $p < 0.05$  was considered statistically significant.

### 3. Results

#### 3.1. Construction of pAd-P311

The sequence of P311-His\_tag was confirmed to be correct by restriction endonuclease reaction (Figure

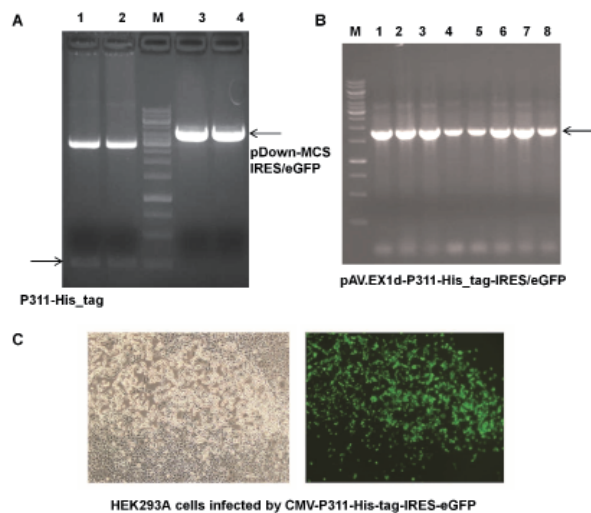


**Figure 1. The construction and identification of Ad P311.** (A) P311-His\_tag (lane 1 and 2) and shuttle vector pDown-MCS-IRES/eGFP (lane 3 and 4) were digested by EcoRI and SpeI (P311-His\_tag fragment about 248 bp, and shuttle vector pDown-MCS-IRES/eGFP about 3.8 kb). Lane M: 1-10 kbp DNA Ladder marker. (B) pAV.EX1d-P311-His\_tag-IRES/eGFP was produced in *E. coli* stb13 cells (lane 1-8, about 1740 bp). (C) HEK293A cells infected by CMV-P311-His-tag-IRES-eGFP. After 8 days infection, the white light and fluorescence were seen ( $\times 100$ ).

1A). Then P311-His\_tag was cloned into shuttle vector pDown-MCS-IRES/eGFP carrying the GFP gene to generate a recombinant plasmid pDown-P311-His\_tag-IRES/eGFP and confirmed to be correct by direct sequencing once again and restriction endonuclease reaction. The pDown-P311-His\_tag-IRES/eGFP and pAV.Des1d were linearized and simultaneously electroporated into host bacteria *E. coli* stb13 cells to generate homologous recombination. The positive clone was identified by sequencing and restriction endonuclease digestion (Figure 1B). The recombinant pAd CMV-P311-His-tag-IRES-eGFP was transferred into HEK293A cells for packaging. When CMV-P311-His\_tag-IRES/eGFP was completely transfected into HEK293A cells for 10 days, the vast majority of cells showed CPE. As shown in Figure 1C, fluorescence and cell change effects were seen after 10 days of post-transfection under the fluorescence microscope. The recombinant pAd CMV-P311-His-tag-IRES-eGFP adenovirus was amplified in HEK293A cells, collected and named Ad-P311. The virus titer of Ad-P311 and Ad-CMV-eGFP was determined to be  $3.675 \times 10^{10}$  TU/mL and  $1.570 \times 10^{10}$  TU/mL, respectively.

### 3.2. The efficiency of infection in NRK-52E cells by recombinant Ad-P311

When different volumes (2  $\mu$ L, 4  $\mu$ L, 6  $\mu$ L, 8  $\mu$ L, 10  $\mu$ L, and 15  $\mu$ L) of Ad-P311 and Ad-CMV-eGFP were respectively transferred into NRK-52E cells for 48h, the efficiency of infection was detected using the inverted fluorescence microscope. After infection by Ad-P311

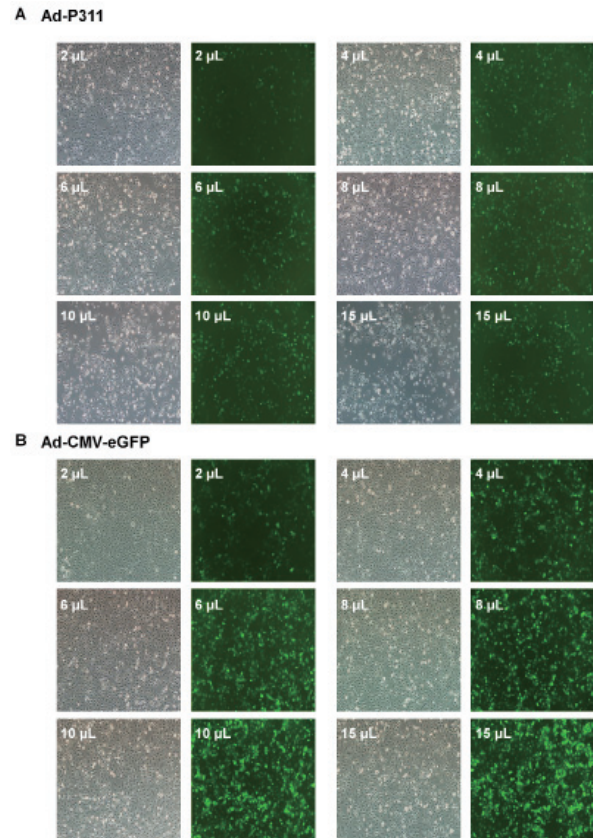


**Figure 2. The efficiency of infection in NRK-52E cells by recombinant Ad-P311.** Different volumes (2  $\mu$ L, 4  $\mu$ L, 6  $\mu$ L, 8  $\mu$ L, 10  $\mu$ L, and 15  $\mu$ L) of Ad-P311 and Ad-CMV-eGFP were respectively transferred into NRK-52E cells for 48h, and the efficiency of infection was detected using the inverted fluorescence microscope ( $\times 100$ ). After infection by Ad-P311 at a volume of 6  $\mu$ L or higher (A), or infection by Ad-CMV-eGFP at a volume of 4  $\mu$ L or higher (B), the transfection rate of NRK-52E cells could reach more than 90%.

at a volume of 6  $\mu$ L or higher, the transfection rate of NRK-52E cells could reach more than 90% (Figure 2A), and the best MOI was 2205. After infection by Ad-CMV-eGFP at a volume of 4  $\mu$ L or higher, the transfection rate of NRK-52E cells also could reach more than 90% (Figure 2B), and the best MOI was 628. These results indicated that the adenovirus-mediated transfection had a high efficiency in NRK-52E cells.

### 3.3. P311 mRNA expression in NRK-52E cells infected by recombinant Ad-P311

After determination of optimal MOI as described above, we then infected NRK-52E cells with Ad-P311 (MOI = 2205). The mRNA expression of P311 in NRK-52E cells infected by recombinant Ad-P311 was detected by quantitative real-time RT-PCR assay. As shown in Figure 3, compared to the NRK-52E group and NRK-52E/GFP group, the mRNA expression of P311 in the NRK-52E/P311 group increased significantly. Furthermore, there is no significant difference between NRK-52E group and NRK-52E/GFP group on mRNA expression of P311. These results showed that P311 was expressed stably in

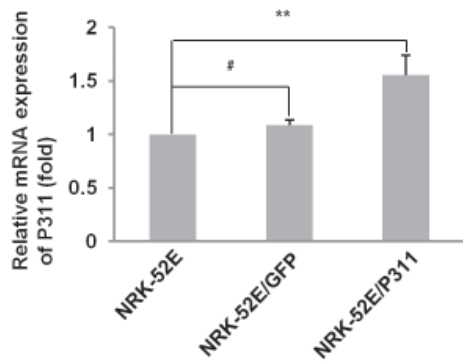


**Figure 3. P311 mRNA expression in NRK-52E cells infected by recombinant Ad-P311.** P311 was expressed stably in NRK-52E cells after being infected with Ad-p311. Compared to the NRK-52E group and NRK-52E/GFP group, the mRNA expression of P311 in the NRK-52E/P311 group increased significantly (\*\* $p < 0.01$ ). There is no significant difference between NRK-52E group and NRK-52E/GFP group on the mRNA expression of P311 ( $p > 0.05$ ).

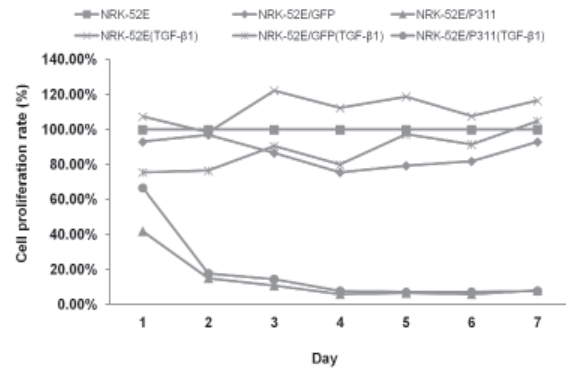


**Figure 4. Growth curve of TGF-β1-induced NRK-52E cells infected by Ad-P311.** P311 had a significant growth-inhibiting effect on NRK-52E cells. Compared to the NRK-52E (TGF-β1) group, the cell proliferation rate in the NRK-52E/P311 (TGF-β1) was decreased significantly.

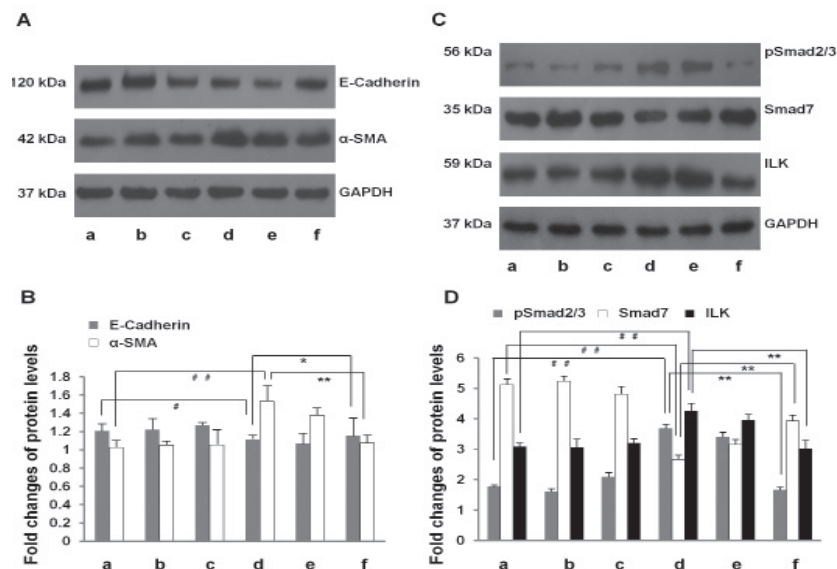


**Figure 5. EMT related proteins expression in TGF-β1-induced NRK-52E cells infected by Ad-P311.** (A) Expression of E-cadherin and α-SMA at the protein level were determined with GAPDH used as an internal control. (B) The expression level of E-cadherin and α-SMA was quantitatively analyzed with Image J software. (C) Expression of pSmad2/3, Smad7, and ILK at the protein level were determined with GAPDH used as an internal control. (D) The expression level of pSmad2/3, Smad7, and ILK was quantitatively analyzed with Image J software. The data show mean ± SD. #  $p < 0.05$ , #  $p < 0.01$ , and #  $p < 0.005$  versus control (NRK-52E group). \*  $p < 0.05$ , \*\*  $p < 0.01$ , and \*\*\*  $p < 0.005$  versus control (NRK-52E (TGF-β1) group). (a: NRK-52E group; b: NRK-52E/GFP group; c: NRK-52E/P311 group; d: NRK-52E(TGF-β1) group; e: NRK-52E/GFP(TGF-β1) group; f: NRK-52E/P311(TGF-β1) group).

NRK-52E cells after being infected with Ad-p311.

### 3.4. Growth curve of TGF-β1-induced NRK-52E cells infected by Ad-P311

MTT assays were performed to investigate the effects of P311 on the proliferation of TGF-β1-induced NRK-52E cells, and a growth curve was drawn according to the results. As shown in Figure 4, after incubation with Ad-P311 for 7 days, P311 had a significant growth-inhibiting effect on the TGF-β1-induced NRK-52E cells. The cell proliferation rate was higher in the NRK-52E (TGF-β1) group than in the NRK-52E group, which indicated that TGF-β1 had the effect of inducing

NRK-52E cell proliferation. Compared to the NRK-52E (TGF-β1) group, the cell proliferation rate in the NRK-52E/P311 (TGF-β1) was decreased significantly, which indicated that P311 could inhibit the proliferation of TGF-β1-induced NRK-52E cells. These results showed that P311 had a significant growth-inhibiting effect on NRK-52E cells.

### 3.5. EMT related proteins expression in TGF-β1-induced NRK-52E cells infected by Ad-P311

To explore the effect of P311 on TGF-β1-induced EMT in NRK-52E cells, the expression of the epithelial marker E-cadherin, and the mesenchymal marker

$\alpha$ -SMA were examined by Western blot analysis. As shown in Figure 5A and 5B, exposure of cells to TGF- $\beta$ 1 resulted in a significant reduction in E-cadherin and an increase in  $\alpha$ -SMA, compared with control. P311 significantly prevented TGF- $\beta$ 1 stimulated changes of E-cadherin and  $\alpha$ -SMA expression. These results suggest that P311 prevents the loss of the epithelial marker E-cadherin and the de novo expression of myofibroblast marker  $\alpha$ -SMA in renal epithelial cells stimulated by TGF- $\beta$ 1.

To explore the possible mechanism of P311 on TGF- $\beta$ 1-induced EMT in NRK-52E cells, the protein expression of EMT related proteins Smad2/3, Smad7, and ILK were measured by Western blot analysis. As shown in Figure 5C and 5D, exposure to TGF- $\beta$ 1 resulted in a significant increase in Smad2/3 phosphorylation and ILK expression, and a significant reduction in Smad7 expression compared with control. Ad-P311 transfection significantly decreased the phosphorylation of Smad2/3 and the expression of ILK in NRK-52E cells compared with TGF- $\beta$ 1-treated group. These results suggest that P311 inhibits TGF- $\beta$ 1-induced EMT in NRK-52E cells *via* regulating the expression of Smad2/3, Smad7 and ILK.

#### 4. Discussion

Although previous work has suggested P311 might be an important factor in myofibroblast transformation and in the progression of fibrosis, the related reports about P311 on renal fibrosis are limited and the mechanism of P311 in the progression of CKD remains largely unknown. EMT plays important roles in accelerating renal fibrosis and promoting the progression of CKD. TGF- $\beta$ 1 is a well-known profibrotic cytokine in several renal diseases and plays a critical role in the renal EMT process. Thus, in the current study, we constructed a recombinant adenovirus vector of p311 and transferred it into NRK-52E cells to explore the preventive effect and possible mechanism of P311 on TGF- $\beta$ 1-induced EMT.

We first successfully constructed recombinant adenovirus vector of P311 (called Ad-P311) and transferred it into rat renal tubular epithelial cells NRK-52E (Figure 1). Then we investigated the effects of Ad-P311 transfection on the biological characteristics of NRK-52E cells. Transfection efficiency of Ad-P311 in NRK-52E cells was evaluated by expression of GFP under the fluorescence microscope (Figure 2). After infection by Ad-P311 at a volume of 6 $\mu$ L or higher, the transfection rate of NRK-52E cells could reach more than 90% and the best MOI was 2205, which indicated that the adenovirus-mediated transfection (Ad-P311) had a high efficiency in NRK-52E cells. To investigate the expression of P311 in NRK-52E cells after transfection, the quantitative real-time RT-PCR assay was performed. Results showed that mRNA expression of P311 was specifically expressed in NRK-52E/P311

cells rather than in NRK-52E cells or NRK-52E/GFP cells (Figure 3). All these findings demonstrate that the P311 gene can be highly and stably transfected into NRK-52E cells with adenovirus mediation.

We investigated the proliferation and growth of P311-expressing cells by MTT assay (Figure 4). From the growth curve of NRK-52E cells, we could see that TGF- $\beta$ 1 had a significant effect on inducing NRK-52E cell proliferation. The cell proliferation rate was higher in the NRK-52E (TGF- $\beta$ 1) group than that in the NRK-52E group. We also could see that P311 had a significant growth-inhibiting effect on the TGF- $\beta$ 1-induced NRK-52E cells. Compared to the NRK-52E (TGF- $\beta$ 1) group, the cell proliferation rate in the NRK-52E/P311 (TGF- $\beta$ 1) group was decreased significantly. All these findings demonstrate that P311 transfection can significantly inhibit the proliferation and growth of TGF- $\beta$ 1 induced NRK-52E cells.

To investigate the possible mechanism by which the P311 gene inhibits cell proliferation and TGF- $\beta$ 1 induced EMT in NRK-52E cells, Western blot analysis was performed to detect the expression of EMT-related proteins and signal pathways. EMT is well known as an important process in the pathogenesis of tubulointerstitial fibrosis and involves a loss of epithelial cell characteristics (loss of E-cadherin) and an increase of mesenchymal cell markers (*e.g.*,  $\alpha$ -SMA). TGF- $\beta$ 1 is identified as the most potent mediator and convergent pathway in inducing EMT and renal fibrosis (23). Here we found that exposure to TGF- $\beta$ 1 for 48 h in NRK-52E cells, E-cadherin expression was decreased and  $\alpha$ -SMA expression was increased significantly (Figure 5A and 5B). However, P311 significantly reverses all of above changes *in vitro* (Figure 5A and 5B). These results suggest that P311 prevents TGF- $\beta$ 1-mediated renal EMT *in vitro*.

TGF- $\beta$ 1/Smads signal pathway has been shown to play a critical role in the process of inducing EMT (7). The Smad family has 8 members forming three subfamilies: the R-Smads (receptor regulated Smads), the Co-Smads (common Smad mediators), and the I-Smads (inhibitory Smads), which are the main TGF- $\beta$  signaling transducers, mediating signaling from cell surface receptors to nuclear target genes (24). Homologous proteins Smad2 and Smad3 belong to the R-Smads, which are highly activated in the fibrotic kidney. It has been demonstrated that activation of TGF- $\beta$ 1 signaling triggers a dramatic induction of Smad2/3 phosphorylation (25). Smad7, as an inhibitory regulator in the TGF- $\beta$ /Smad signaling pathway, can be induced by TGF- $\beta$ 1 to block the overactivation of TGF- $\beta$  signals *via* its negative feedback loop. TGF- $\beta$  not only induces Smad7 transcription, but also promotes the degradation of Smad7 *via* the Smad3-dependent Smurfs/arkadia-mediated ubiquitin-proteasome degradation pathway (26). In this study, we investigated the effects of P311 on the TGF- $\beta$ 1/

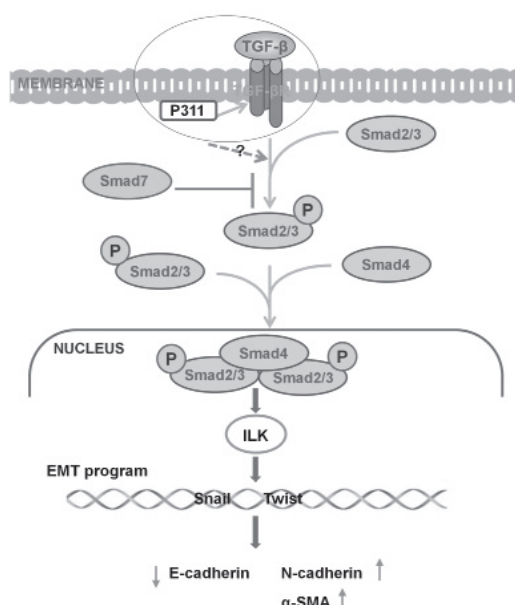


**Figure 6.** The possible mechanisms of P311 involved in the TGF- $\beta$ 1-induced EMT process in renal fibrosis via TGF- $\beta$ 1-Smad-ILK pathway.

Smads signal pathway in NRK-52E cells. Here we found that exposure to TGF- $\beta$ 1 for 48 h in NRK-52E cells, p-Smad2/3 expression was increased and Smad7 expression was decreased significantly (Figure 5C and 5D). However, P311 significantly reverses all of the above changes *in vitro* (Figure 5C and 5D). Our results showed that P311 inhibited p-Smad2/3 activation and promoted Smad7 activation induced by TGF- $\beta$ 1 in NRK-52E cells. We also further studied the effects of P311 on ILK expression, which was the important downstream mediator of TGF- $\beta$ 1/Smads signaling pathway. ILK has shown to be a key intracellular mediator that controls TGF- $\beta$ 1-induced-EMT in renal tubular epithelial cells (9). Here we found that exposure to TGF- $\beta$ 1 for 48 h in NRK-52E cells, ILK expression was increased significantly (Figure 5C and 5D), however, P311 significantly reverses the above changes *in vitro* (Figure 5C and 5D). These results showed that infection of P311 in NRK-52E cells attenuated TGF- $\beta$ 1-induced upregulation of ILK expression.

In conclusion, our data present that P311 could block TGF- $\beta$ 1-induced EMT probably by inhibiting the activation of p-Smad2/3 and ILK and promoting the activation of Smad7 in NRK-52E cells. These findings suggest that P311 might be involved in the pathogenesis of renal fibrosis by inhibiting the EMT process *via* the TGF- $\beta$ 1-Smad-ILK pathway (Figure 6). P311 might be a novel target for control of renal fibrosis and progression of CKD.

#### Acknowledgements

The current work was supported by the National Natural Science Foundation of China (No. 81273682)

and the Science and Technology Development Program of Shandong Province (No. 2010G0020220).

#### References

1. Tonelli M, Wiebe N, Culleton B, House A, Rabbat C, Fok M, McAlister F, Garg AX. Chronic kidney disease and mortality risk: A systematic review. *J Am Soc Nephrol.* 2006; 17:2034-2047.
2. Boor P, Ostendorf T, Floege J. Renal fibrosis: Novel insights into mechanisms and therapeutic targets. *Nat Rev Nephrol.* 2010; 6:643-656.
3. Liu Y. New insights into epithelial-mesenchymal transition in kidney fibrosis. *J Am Soc Nephrol.* 2010; 21:212-222.
4. Kriz W, Kaissling B, Le Hir M. Epithelial-mesenchymal transition (EMT) in kidney fibrosis: Fact or fantasy? *J Clin Invest.* 2011; 121:468-474.
5. Guo Y, Li Z, Ding R, Li H, Zhang L, Yuan W, Wang Y. Parathyroid hormone induces epithelial-to-mesenchymal transition *via* the Wnt/ $\beta$ -catenin signaling pathway in human renal proximal tubular cells. *Int J Clin Exp Pathol.* 2014; 7:5978-5987.
6. Wang Q, Wang Y, Huang X, Liang W, Xiong Z, Xiong Z. Integrin  $\beta$ 4 in EMT: An implication of renal diseases. *Int J Clin Exp Med.* 2015; 8:6967-6976.
7. Sun S, Sun W, Xia L, Liu L, Du R, He L, Li R, Wang H, Huang C. The T-box transcription factor Brachyury promotes renal interstitial fibrosis by repressing E-cadherin expression. *Cell Commun Signal.* 2014; 12:76.
8. Jia L, Ma X, Gui B, Ge H, Wang L, Ou Y, Tian L, Chen Z, Duan Z, Han J, Fu R. Sorafenib ameliorates renal fibrosis through inhibition of TGF- $\beta$ -induced epithelial-mesenchymal transition. *PLoS One.* 2015; 10:e0117757.
9. Kim MK, Maeng YI, Sung WJ, Oh HK, Park JB, Yoon GS, Cho CH, Park KK. The differential expression of TGF- $\beta$ 1, ILK and wnt signaling inducing epithelial to mesenchymal transition in human renal fibrogenesis: An immunohistochemical study. *Int J Clin Exp Pathol.* 2013; 6:1747-1758.
10. Li Y, Yang J, Dai C, Wu C, Liu Y. Role for integrin-linked kinase in mediating tubular epithelial to mesenchymal transition and renal interstitial fibrogenesis. *J Clin Invest.* 2003; 112:503-516.
11. Penn JW, Grobbelaar AO, Rolfe KJ. The role of the TGF- $\beta$  family in wound healing, burns and scarring: A review. *Int J Burns Trauma.* 2012; 2:18-28.
12. Paliwal S, Shi J, Dhru U, Zhou Y, Schuger L. P311 binds to the latency associated protein and downregulates the expression of TGF-beta1 and TGF-beta2. *Biochem Biophys Res Commun.* 2004; 315:1104-1109.
13. Pan D, Zhe X, Jakkaraju S, Taylor GA, Schuger L. P311 induces a TGF-beta1-independent, nonfibrogenic myofibroblast phenotype. *J Clin Invest.* 2002; 110:1349-1358.
14. Mariani L, McDonough WS, Hoelzinger DB, Beaudry C, Kaczmarek E, Coons SW, Giese A, Moghaddam M, Seiler RW, Berens ME. Identification and validation of P311 as a glioblastoma invasion gene using laser capture microdissection. *Cancer Res.* 2001; 61:4190-4196.
15. Fujitani M, Yamagishi S, Che YH, Hata K, Kubo T, Ino H, Tohyama M, Yamashita T. P311 accelerates nerve regeneration of the axotomized facial nerve. *J*

- Neurochem. 2004; 91:737-744.
16. Zhao L, Leung JK, Yamamoto H, Goswami S, Kheradmand F, Vu TH. Identification of P311 as a potential gene regulating alveolar generation. *Am J Respir Cell Mol Biol.* 2006; 35:48-54.
  17. Tan J, Peng X, Luo G, Ma B, Cao C, He W, Yuan S, Li S, Wilkins JA, Wu J. Investigating the role of P311 in the hypertrophic scar. *PLoS One.* 2010; 5:e9995.
  18. Wang F, Xie X, Fan J, Wang L, Guo D, Yang L, Ma X, Zhang L, Li Z. Expression of P311, a transforming growth factor beta latency-associated protein-binding protein, in human kidneys with IgA nephropathy. *Int Urol Nephrol.* 2010; 42:811-819.
  19. Liu D, Hu L, Zhang Z, Li QY, Wang G. Construction of human BMP2-IRES-HIF1 $\alpha$  adenovirus expression vector and its expression in mesenchymal stem cells. *Mol Med Rep.* 2013; 7:659-663.
  20. Zhao YN, Li Q. Adenovirus mediated BIMS transfer induces growth suppression and apoptosis in Raji lymphoma cells. *Biomed Environ Sci.* 2014; 27:655-664.
  21. Yin Y, Qi F, Song Z, Zhang B, Teng J. Ferulic acid combined with astragaloside IV protects against vascular endothelial dysfunction in diabetic rats. *Biosci Trends.* 2014; 8:217-226.
  22. Cui XY, Inagaki Y, Wang DL, Gao JJ, Qi FH, Gao B, Kokudo N, Fang DZ, Tang W. The supercritical CO<sub>2</sub> extract from the skin of *Bufo bufo gargarizans* Cantor blocks hepatitis B virus antigen secretion in HepG2.2.15 cells. *BioScience Trends.* 2014; 8:38-44.
  23. Lamouille S, Xu J, Derynck R. Molecular mechanisms of epithelial-mesenchymal transition. *Nat Rev Mol Cell Biol.* 2014; 15:178-196.
  24. Tirado-Rodriguez B, Ortega E, Segura-Medina P, Huerta-Yepez S. TGF- $\beta$ : An important mediator of allergic disease and a molecule with dual activity in cancer development. *J Immunol Res.* 2014; 2014:318481.
  25. Meng XM, Chung AC, Lan HY. Role of the TGF- $\beta$ /BMP-7/Smad pathways in renal diseases. *Clin Sci (Lond).* 2013; 124:243-254.
  26. Meng XM, Tang PM, Li J, Lan HY. TGF- $\beta$ /Smad signaling in renal fibrosis. *Front Physiol.* 2015; 6:82.
- (Received September 29, 2015; Revised October 12, 2015; Accepted October 15, 2015)